Simon, H., Buske, S., Hedin, P., Juhlin, C., Krauß, F., Giese, R. (2019): Anisotropic Kirchhoff pre-stack depth migration at the COSC-1 borehole, central Sweden. - *Geophysical Journal International*, *219*, 1, pp. 66—79.

DOI: http://doi.org/10.1093/gji/ggz286

Geophysical Journal International

Geophys. J. Int. (2019) **219,** 66–79
Advance Access publication 2019 June 24
GJI Seismology

doi: 10.1093/gji/ggz286

Anisotropic Kirchhoff pre-stack depth migration at the COSC-1 borehole, central Sweden

H. Simon,[1] S. Buske,[1] P. Hedin,[2,*] C. Juhlin,[2] F. Krauß[3] and R. Giese[3]

[1] *Institute of Geophysics and Geoinformatics, TU Bergakademie Freiberg, D-*09596 *Freiberg, Germany. E-mail: helge.simon@geophysik.tu-freiberg.de*
[2] *Department of Earth Sciences, Uppsala University,* 75236 *Uppsala, Sweden*
[3] *Centre for Scientific Drilling, GFZ German Research Centre for Geosciences - Helmholtz Centre Potsdam, D-*14473 *Potsdam, Germany*

Accepted 2019 June 19. Received 2019 May 24; in original form 2018 October 30

SUMMARY

A remarkably well preserved representation of a deeply eroded Palaeozoic orogen is found in the Scandinavian Caledonides, formed by the collision of the two palaeocontinents Baltica and Laurentia. Today, after 400 Ma of erosion along with uplift and extension during the opening of the North Atlantic Ocean, the geological structures in central western Sweden comprise far transported allochthonous units, the underlying Precambrian crystalline basement, and a shallow west-dipping décollement that separates the two and is associated with a thin layer of Cambrian black shales. These structures, in particular the Seve Nappes (upper part of the Middle Allochthons), the Lower Allochthons and the highly reflective basement are the target of the two approximately 2.5 km deep fully cored scientific boreholes in central Sweden that are part of the project COSC (Collisional Orogeny in the Scandinavian Caledonides). Thus, a continuous 5 km tectonostratigraphic profile through the Caledonian nappes into Baltica's basement will be recovered. The first borehole, COSC-1, was successfully drilled in 2014 and revealed a thick section of the seismically highly reflective Lower Seve Nappe. The Seve Nappe Complex, mainly consisting of felsic gneisses and mafic amphibolites, appears to be highly anisotropic. To allow for extrapolation of findings from core analysis and downhole logging to the structures around the borehole, several surface and borehole seismic experiments were conducted. Here, we use three long offset surface seismic profiles that are centred on the borehole COSC-1 to image the structures in the vicinity of the borehole and below it. We applied Kirchhoff pre-stack depth migration, taking into account the seismic anisotropy in the Seve Nappe Complex. We calculated Green's functions using an anisotropic eikonal solver for a VTI (transversely isotropic with vertical axis of symmetry) velocity model, which was previously derived by the analysis of VSP (Vertical Seismic Profile) and surface seismic data. We show, that the anisotropic results are superior to the corresponding isotropic depth migration. The reflections appear significantly more continuous and better focused. The depth imaging of the long offset profiles provides a link between a high-resolution 3-D data set and the regional scale 2-D COSC Seismic Profile and complements these data sets, especially in the deeper parts below the borehole. However, many of the reflective structures can be observed in the different data sets. Most of the dominant reflections imaged originate below the bottom of the borehole and are situated within the Precambrian basement or at the transition zones between Middle and Lower Allochthons and the basement. The origin of the deeper reflections remains enigmatic, possibly representing dolerite intrusions or deformation zones of Caledonian or pre-Caledonian age.

Key words: Composition and structure of the continental crust; Controlled source seismology; Crustal imaging; Seismic anisotropy; Crustal structure.

* Now at: Department of Mineral Resources, Geological Survey of Sweden, 752 36 Uppsala, Sweden.

1 INTRODUCTION

The deep erosion of the Palaeozoic Scandinavian mountain belt and the lack of a recent orogenic overprint makes the Scandinavian Caledonides a unique area to study mountain building processes, such as thrust and extensional tectonics (e.g. Gee 1975, 1978; Andersen 1998) and to relate these processes to active mountain belts, like the Himalayas (e.g. Streule *et al.* 2010). The project COSC (Collisional Orogeny in the Scandinavian Caledonides) within the framework of the International Continental scientific Drilling Programm (ICDP) examines the structure and physical conditions of the Scandinavian orogenic units and the underlying Precambrian basement with the aim to further deepen our understanding of orogenic processes in the past (Caledonian Orogeny) and in active mountain belts (e.g. the Himalayas). This will be achieved by two approximately 2.5 km deep fully cored scientific boreholes in central Sweden and the associated research on the core material, logging data and additional geological and geophysical field surveys (e.g. seismics, magnetotellurics).

The first drillhole COSC-1 (IGSN: http://hdl.handle.net/10273/ICDP5054EHW1001) was drilled and fully cored to a depth of 2.5 km in 2014 near the town of Åre (Lorenz *et al.* 2015) and targeted the lower parts of the high-grade Seve Nappe Complex (SNC). The second drillhole COSC-2, located approximately 20 km further to the east and planned for 2020, will start in the underlying lower grade allochthons and aims to penetrate the main décollement and at least one of the basement reflectors. Both boreholes together will reveal an approximately 5-km-long tectonostratigraphic sequence through the Caledonian nappes of the Middle and Lower Allochthons and the Precambrian Basement.

The drilling of COSC-1 was complemented by seismic surveys in order to characterize the direct vicinity of the borehole and to relate findings from the drill core and logging data to the surrounding structures known from, for example regional scale seismic profiles. The seismic investigations included borehole [zero-offset and multiazimuthal walkaway Vertical Seismic Profile (VSP)] and surface based (long offset profiles and a spatially limited 3-D survey) experiments and were conducted right after the drilling of COSC-1 was completed.

Here, we use three long offset surface seismic profiles centred on COSC-1 to image structures around and in particular below the borehole. We used an anisotropic Kirchhoff pre-stack depth migration approach in order to account for the strong anisotropy in the Seve Nappe Complex that was detected by laboratory measurements on COSC-1 core samples (Wenning *et al.* 2016) and the analysis of first arrivals from the VSP and surface data, and which can be described by a VTI (transversely isotropic with vertical axis of symmetry) velocity model (Simon *et al.* 2017). With this approach we were able to produce clear images of the reflective structures around and below the borehole. These results fill a gap with respect to survey geometry and resolution between the high-resolution 3-D data (Hedin *et al.* 2016) and the regional scale 2-D COSC Seismic Profile (CSP, Juhlin *et al.* 2016). We were able to link many reflectors that are imaged in our results to structures found in the CSP and the 3-D data set and vice versa. Additionally, we demonstrate the necessity to account for anisotropy also in crystalline environments by comparing the anisotropic imaging results to the depth migration using a corresponding isotropic velocity model.

2 GEOLOGY AND GEOPHYSICS OF THE AREA

2.1 Geological setting

The Caledonian orogeny affected large parts of today's North Atlantic continental margins. Remnants of this Palaeozoic orogen can be found in the northern parts of Great Britain, the Scandinavian Mountains, Svalbard, eastern Greenland, parts of north-central Europe as well as parts of eastern North America. The mountain building of the Caledonian orogeny was caused by the closure of the Iapetus Ocean in the Early Silurian and the subsequent collision of the palaeocontinents Baltica and Laurentia, including underthrusting of Baltica beneath Laurentia. The Cenozoic opening of the North Atlantic together with about three hundred million years of erosion, uplift and extension, exposed rocks of former mid-crustal levels at the surface of Norway and western Sweden. Therefore, the Scandinavian Caledonides represent a unique site to study orogenic processes.

A comprehensive summary about the Scandinavian Caledonides can be found in Gee & Sturt (1985), while the major scientific discoveries of the last decades are presented in Corfu *et al.* (2014).

Today, the Scandinavian Caledonides represent a stack of nappes emplaced from west to east onto the margins of Baltica during the collison with Laurentia 440–400 Ma ago (Gee *et al.* 2008). They have usually small vertical thickness but wide lateral extent. The allochthonous nappes can be subdivided in four major groups (Lower, Middle, Upper and Uppermost Allochthons; according to Gee & Sturt 1985) according to their origin on one or the other palaeocontinent. All of the Scandinavian allochthons are folded by major N–S trending synforms (e.g. Tännforsen, Åre) and antiforms (e.g. Mullfjället, Olden-Öviksfjället) that are related to crustal extension and normal faulting after or during the final stages of the orogen (see Fig. 1).

The nappes in the study area of COSC belong to the Middle and Lower Allochthons and contain mainly sedimentary and metamorphic rocks. They are mapped and illustrated by Strömberg *et al.* (1984). Their work also provides the base for the map shown in Fig. 1.

The Middle Allochthons consist of a basal basement-derived thrust sheet, overlain by metasandstones, the Särv and Offerdal Nappes, and the lower units of the Seve Nappe Complex as the uppermost tectonic unit in the Middle Allochthons. The Lower Seve Nappe was the main target of the COSC-1 borehole. This unit consists of mainly felsic (gneisses) and mafic (amphibolites) lithologies. In the deeper parts also micaschists are more frequent. The Lower Allochthon, also called the Jämtlandian Nappes, comprises Cambrian quartzites and shales, Ordovician limestones and Ordovician to Silurian turbidites (greywackes) that are alternating along the detachment. The Caledonian Allochthons at the thrust front are separated from the underlying Precambrian crystalline basement by a major 1–2° west-dipping décollement. The Proterozoic crystalline basement below the Caledonian nappes is probably deeply deformed (Juhojuntti *et al.* 2001) and seismically highly reflective. Two possibilities for the strong reflectivity have been discussed (Palm *et al.* 1991; Juhojuntti *et al.* 2001), which are deformation zones of Caledonian or pre-Caledonian age or mafic (dolerite) intrusions into the mainly granitic basement.

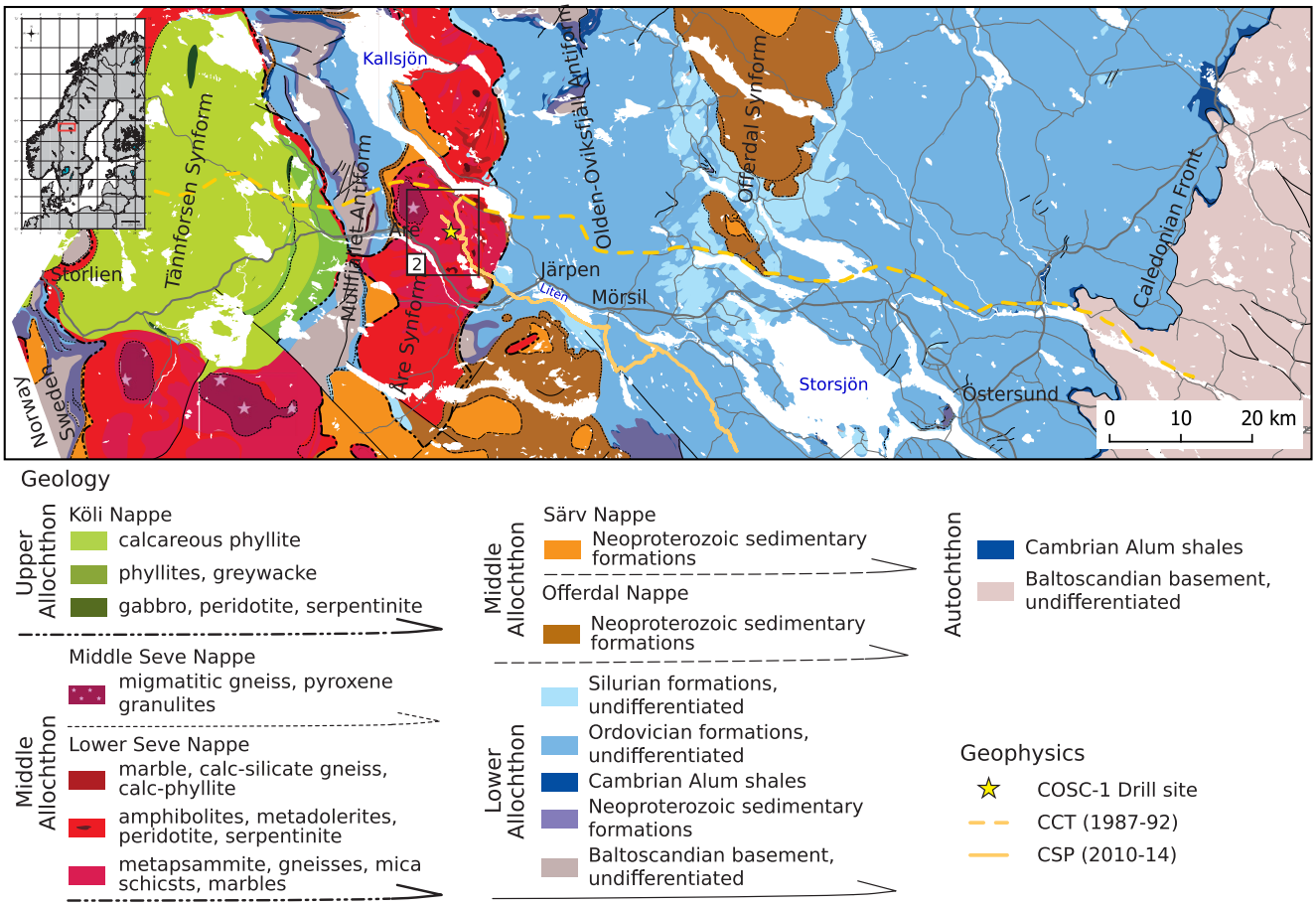

Figure 1. Regional geological map (after Hedin *et al.* (2016), based on the bedrock map of Sweden, © Geological Survey of Sweden (I2014/00601) and Strömberg *et al.* (1984)) showing the different allochthonous nappes and the autochthonous basement in the central Scandinavian Caledonides. The regional scale seismic profiles (CCT, CSP) and the COSC-1 drillsite are marked. The black rectangle indicates the location of the map in Fig 2.

2.2 Previous geophysical investigations

Geophysical investigations in the Scandinavian Caledonides began in the 1970s (Gee & Sturt 1985) and have continued until today (e.g. see Corfu *et al.* 2014). The Central Caledonian Transect (CCT), a profile crossing the mountain belt from the coast of Norway to Östersund in central Sweden, has played a key role during these investigations (Dyrelius *et al.* 1980). Along this profile a major reflection seismic survey was conducted, which imaged the entire crust down to the Moho and provided images of the crustal structures related to the Caledonian deformation (Hurich *et al.* 1989; Palm *et al.* 1991; Juhojuntti *et al.* 2001). The CCT shows a very reflective upper crust and transparent zones in the lower crust. The reflectivity pattern indicates crustal shortening which is consistent with observations visible at the surface, for example the folding in major N–S striking antiforms and synforms. Strong reflections in the east can be projected to the surface where old dolerite intrusions are found in the surface geology. Further to the south, in the Siljan Ring area, similar reflection patterns could be linked by drilling to a set of dolerite intrusions (Juhlin 1990). Therefore, the strong reflections seen in the CCT seismic profile might be due to the contrast between the granitic host rocks of the basement and dolerite intrusions. Nevertheless, deformation zones of Caledonian or pre-Caledonian age or a combination of both (mafic intrusions and orogenic deformation), may also be an explanation for this reflectivity. In addition, a gently west-dipping reflection was detected (although not continuously), which can be traced from the surface outcrop of the Caledonian front to the Swedish-Norwegian border at a depth of approximately 7 km. This was interpreted by Palm *et al.* (1991) as the sole thrust, that is the lower limit of Caledonian deformation including both, the allochthons and the underlying crystalline basement. Another thrust zone was defined, here referred to as the main (Jämtlandian) décollement, that separates the overlying transported allochthons from the underlying less deformed basement (Juhlin *et al.* 2016). The sole thrust defined in the CCT ramps up in the eastern part into the main décollement. Magnetotelluric measurements along the Swedish part of the profile (Korja *et al.* 2008) further support this interpretation. They show a highly conductive layer with a well defined upper boundary on top of a resistive layer. The boundary was interpreted as the main décollement which is also associated with highly conductive alum shales.

With the beginning of the COSC project (Gee *et al.* 2010), the seismic reflection profile CSP (COSC Seismic Profile, Fig. 1) was acquired (Hedin *et al.* 2012; Juhlin *et al.* 2016) with the purpose of finding the most suitable locations for the two COSC boreholes. Complementary, a magnetotelluric survey was conducted along the same profile (Yan *et al.* 2017a). These profiles allowed a detailed geological interpretation of the major tectonic structures of the upper approximately 10 km of the crust. While Hedin *et al.* (2012) interpreted a deeper fairly continuous reflection in the seismic section as the main décollement that separates the allochthons from

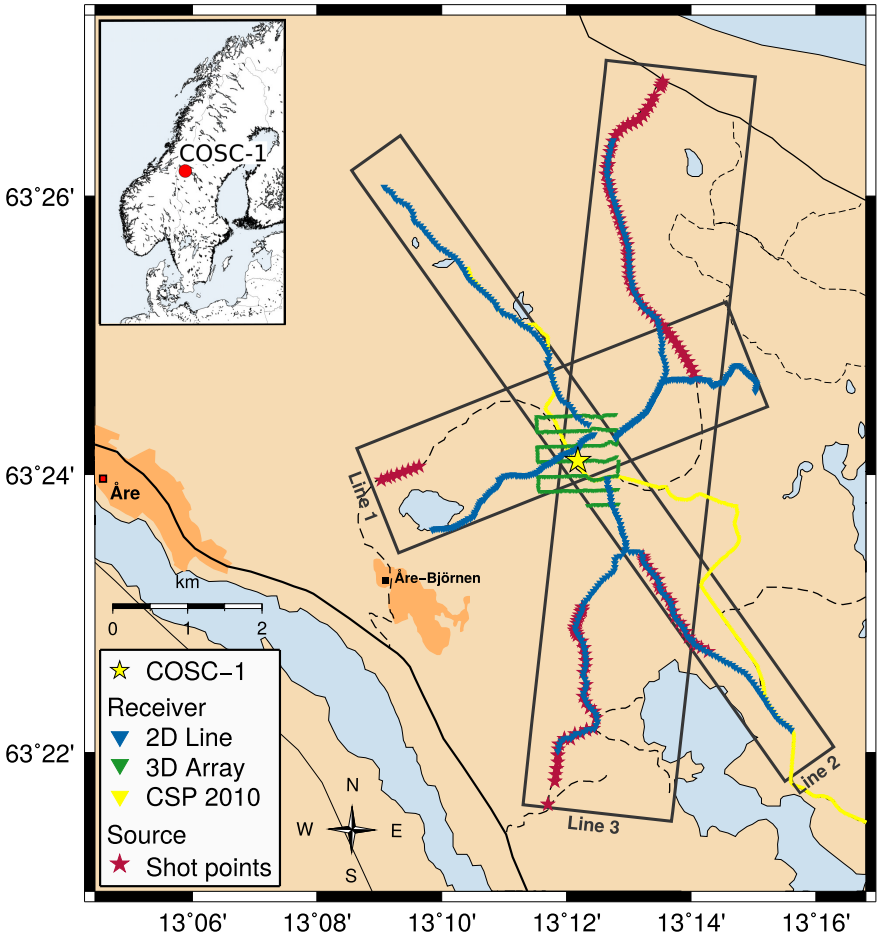

Figure 2. Seismic source (red) and receiver (blue) positions of the three surface profiles centred around the borehole COSC-1 (yellow star). The 3-D receiver array (green) recorded the same source positions. The north-western part of the previously aquired COSC Seismic Profile (CSP) is marked in yellow.

the basement, Juhlin *et al.* (2016) presented an alternative shallower décollement surface, also with regard to the magnetotelluric results which proved the conductive alum shales to be located much shallower (Yan *et al.* 2017a,b). This interpretation is supported by another laterally continuous seismic reflection.

A highly reflective unit, reaching a depth of approximately 2.3 km in the western part of the CSP profile, was interpreted from the seismic section as the Seve Nappe Complex (SNC, Hedin *et al.* 2012). To the east, the base of the SNC rapidly becomes shallower and thins out to the surface about 10 km east of the town Åre. Only very little information about the internal and underlying structures of the SNC could be extracted from the surface reflection data, probably due to the small-scale complex internal 3-D geometry and strong scattering of the seismic energy (Hedin 2015).

The target for COSC-1 was to investigate the lower units of the high-grade Seve Nappe Complex. Therefore, a drillsite in the eastern flanks of the Åreskutan synform near the town of Åre was chosen. With its depth of 2.5 km COSC-1 penetrated the SNC and probably reached a transition zone to the underlying units. The lithological description of the drill core shows mainly alternating layers of felsic calc-silicates/gneisses and amphibolites in the uppermost approximately 1700 m. Below this depth an approximately 800-m-thick shear zone, where mylonites occur with increasing frequency and thickness, was encountered. Below depths of 2350 m, lower grade mylonitized metasandstones are present, that could belong to underlying units, here especially the Särv Nappe.

After drilling of COSC-1 was completed, borehole based seismic investigations were conducted. These included several components: zero-offset VSP, multi-azimuthal walkaway VSP, a spatially limited 3-D survey and three long offset surface profiles centred on the borehole. With these investigations an area of approximately 5 km × 10 km around the borehole was covered in order to image structures in the direct vicinity of the borehole, as well as below it, and to allow an extrapolation of findings from the core and the logging data to the surrounding formation.

Through the analysis of the 3-D data recorded by an array of vertical component geophones in the central part of the survey area, covering an area of about 1.5 km^2, Hedin *et al.* (2016) were able to image the internal structure of the SNC and some of the underlying reflectors and link them to the previous results from the CSP. It appears that the SNC has a very complex 3-D geometry and lithology with varying dips in different directions and, especially in the uppermost part, a low lateral continutity of the reflections. This is further supported by the analysis of zero-offset VSP data by Krauß (2018), who linked a corridor stack derived from the zero-offset VSP to the surface 3-D data and the borehole logs. Reflections associated with the interpreted shear zone at the base of the SNC appear more continuous and generally well defined.

Simon *et al.* (2017) used the multi-azimuthal walkaway VSP data in combination with the long offset surface data to derive a velocity model for the vicinity of the COSC-1 borehole. They showed that the SNC is highly anisotropic. Consequently, they constructed a

model that considers different velocities for seismic rays travelling in vertical and horizontal direction.

In this paper we complement the existing results of this survey and the previous investigations, like the CSP, by using data recorded along three surface profiles, azimuthally centred on the COSC-1 borehole, to image structures around, and especially below the borehole and the SNC. For that we used a Kirchhoff pre-stack depth migration approach and the anisotropic velocity model derived by Simon *et al.* (2017).

3 DATA AND METHODS

3.1 Data

The borehole based seismic survey was conducted directly after the drilling of COSC-1 was completed in autumn 2014. The survey consisted of several separate experiments, which were partly linked through recording the seismic wavefield generated at the same source points. The first component was a zero-offset VSP with dense receiver spacing along the entire borehole (Krauß 2018). The second part consisted of a combination of three long offset surface profiles along different azimuths and centred on the borehole and a multi-azimuthal walkaway VSP survey (for more acquisition details see Simon *et al.* 2017). The last part was a limited 3-D survey, consisting of 429 receivers deployed in an array around the COSC-1 borehole in the central part of the survey area, which recorded the same shot positions used for the second survey part (Hedin *et al.* 2016).

In this study, we used a subset of the shot points along the three surface profiles as shown in Fig. 2. These shots were recorded by 180 three-component receivers along each of the three up to 10-km-long profiles. The profiles themselves are strongly crooked due to the difficult terrain and limited accessibility, and the distribution of shot points and receiver positions is rather irregular and partly very sparse. In addition, the profiles exhibit a strong topography. A summary of the acquisition parameters can be found in Table 1. Small explosions (0.5 kg charge) were fired in shallow shotholes (3–5 m deep) filled with water to allow for a second use and, when possible they were fired for a second time filled with gravel to increase the downwards emitted seismic energy. Such a possibility for a second shot firing was possible for approximately 60 per cent of the shot holes. For logistical reasons the first shooting along line 1 was recorded by the receivers deployed along line 2 and the reshooting was recorded along line 1. For the shooting along line 2 the situation was vice versa. Here the first shooting was recorded along line 2 and the reshooting along line 1. For line 3 both shootings were recorded along the same line 3. The receiver spacing was approximately 50 m (30 m for line 1) and the nominal shot point spacing was 80 m, covering mostly only small parts of the particular profile. On line 1 only 8 shot positions in the far west of the profile and an additional offset to the north of the receiver line were fired. For line 2 only 22 shot positions in the southeastern part were used. Line 3 has a significantly better coverage with 105 shot positions in the northern and southern part of the profile. For the walkaway VSP and the 3-D survey the gaps in the central part of the survey area were filled with another source type, the VIBSIST system (Park *et al.* 1996; Cosma & Enescu 2001; Juhlin *et al.* 2010). Unfortunately the signal-to-noise ratio of the corresponding shot gathers was comparably low, so that they were not used here in this study.

3.2 Pre-processing

The pre-processing (i.e. all processing steps prior to pre-stack depth migration) of the data followed a standard processing sequence (see Table 2) in order to enhance the signal of the reflected waves and to suppress unwanted signals and noise. Every shot gather was checked visually and dead or very noisy traces were killed manually. High amplitude arrivals of the direct/refracted waves were suppressed by a top mute manually defined for each shot gather. Spiking deconvolution (Wiener–Levinson) with an operator length of 150 ms helped to sharpen the signals. Different filters like spectral shaping, a time variant bandpass and an automatic gain control further improved the signal-to-noise ratio of the data. Fig. 3(left-hand panel) shows a typical raw shot gather from one of the southernmost shot points on line 2. Already in this raw shot gather several clear reflections can be observed. Fig. 3(right-hand panel) shows the same shot gather after the above described processing sequence. The reflections stand out much clearer and can be traced over the entire offset range together with additional previously obscured reflections which were not directly visible in the raw shot gather.

3.3 Anisotropic velocity model

The first step in seismic pre-stack depth imaging is the derivation of an appropriate migration velocity model, which is necessary to produce reliable images of the structures. Simon *et al.* (2017) investigated the velocity distribution of the Seve Nappe Complex (SNC) in the vicinity of the COSC-1 borehole. The study was based on a combined evaluation of the multi-azimuthal walkaway VSP data recorded in the borehole as well as on the surface along different azimuths around the borehole. The comparison of velocities derived from mainly horizontally travelling waves (recorded along the surface) with velocities obtained from mainly vertically travelling waves recorded in the borehole as part of the zero-offset VSP component showed that the SNC is characterized by strong seismic anisotropy and that an isotropic velocity model cannot explain first arrival traveltimes from both, VSP and surface seismic data at once. However, using an anisotropic VTI (transversely isotropic with vertical axis of symmetry) velocity model the traveltimes from all survey components could be explained very well. This VTI model is defined by a vertical *P*-wave velocity function directly derived from zero-offset VSP interval velocities and spatially constant Thomsen parameters $\epsilon = 0.03$ and $\delta = 0.3$ derived from laboratory studies (Wenning *et al.* 2016) and estimated from the analysis of surface seismic and far offset VSP data (Simon *et al.* 2017).

We used this VTI model as the base for constructing a migration velocity model as input to our pre-stack depth migration approach. Since the VTI model was derived by Simon *et al.* (2017) only down to a depth of 2.5 km, it had to be extended towards greater depths from which we observe reflections in our data set. For the part below the Seve Nappes, that is for the Lower Allochthons and the Precambrian basement, we used a constant value of 5.9 km s^{-1} to extend the VTI velocity model towards a final model depth of 9 km. This velocity value corresponds to the mean velocity in the lower part of the vertical velocity function from the zero-offset VSP (Krauß 2018). A slightly increasing velocity with depth might be more realistic, but since we do not have any information about the potential velocity gradient, we assumed here a constant velocity. We expect the Lower Allochthons and the basement to be not or only slightly anisotropic. Therefore, the Thomsen parameters below 2.5 km depth, that is below the Seve Nappes, were set to zero. Thus, the final migration velocity model consists of a 2.5-km-thick

Table 1. Acquisition source and receiver parameters for the three surface profiles (see also Fig. 2).

	Line 1	Line 2	Line 3
Source points	8	22	105
Excitation/source point	1–2	1–2	1–2
Nominal source spacing	80 m	80 m	80 m
Explosive charge	0.5 kg	0.5 kg	0.5 kg
Explosive charge depth	3 m	5 m	5 m
Shothole filling	water/gravel	water/gravel	water/gravel
Number of receivers	180	180	180
Receiver type	4.5 Hz, 3C	4.5 Hz, 3C	4.5 Hz, 3C
Receiver spacing	30 m	50 m	50 m
Recording instruments	Omnirecs DATA-CUBE^3	Omnirecs DATA-CUBE^3	Omnirecs DATA-CUBE^3
Sampling interval	2.5 ms	2.5 ms	2.5 ms
Record length	Continuous recording	Continuous recording	Continuous recording

Table 2. Processing parameters for all processing steps applied prior to pre-stack depth migration.

Trace editing	Manual
Topmute	Manually defined
Wiener–Levinson deconvolution	Minimum phase spiking,150 ms operator length
Spectral shaping	15–30–100–180 Hz
Bandpass filter (time variant)	0–700 ms: 25–50–140–210 Hz 1000–1400 ms: 20–40–120–180 Hz 1600–5000 ms: 20–40–100–150 Hz
Automatic gain control	rms, time window 400 ms

anisotropic VTI layer and a homogeneous isotropic layer with a constant velocity of 5.9 km s^{-1} below.

3.4 Anisotropic Kirchhoff pre-stack depth migration

In order to obtain reliable images of structures in the subsurface from seismic reflections recorded at the surface, these have to be traced back to their correct position at depth. This backpropagation of the wavefield can be achieved by migration techniques. The method we used here, is the well established Kirchhoff Pre-Stack Depth Migration (KPSDM). Anisotropic KPSDM is widely used in sedimentary environments, however in hard rock seismic applications it is not yet state of the art. Therefore, in the following we briefly describe the theory behind it.

Since KPSDM is usually implemented as a weighted stack of the traveltime isochrones, traveltime information for shot and receiver positions are required to construct the diffraction surfaces. Mostly these traveltimes are calculated numerically using a finite difference eikonal solver (e.g. Podvin & Lecomte 1991). We used an anisotropic finite difference eikonal solver (Riedel 2016) which is capable of calculating first arrival traveltimes in general transversely isotropic (TI) media. This algorithm solves the eikonal equation using the Fast Marching Method (Sethian & Popovici 1999; Sethian 2001). This algorithm imitates Huygens' principle and ensures causality of the first arrival traveltime computation.

In the anisotropic case, the velocity in the eikonal equation has to be replaced by the respective anisotropic phase velocity, in our case the phase velocity of the *P*-wave. In anisotropic media the phase velocity depends on the propagation direction and the dependence on the elastic moduli is more complicated than in the isotropic case. Thomsen (1986) introduced a parametrization for weak anisotropy in TI media. With this convention, the phase velocity of the *P*- wave can be described by only three independent parameters, namely the vertical *P*-wave phase velocity v_{P0}, and the two Thomsen parameters ϵ and δ:

$$v_{P0} = \sqrt{\frac{c_{33}}{\rho}} \tag{1}$$

$$\epsilon = \frac{c_{11} - c_{33}}{2c_{33}} \tag{2}$$

$$\delta = \frac{(c_{13} + c_{44})^2 - (c_{33} - c_{44})^2}{2c_{33}(c_{33} - c_{44})}. \tag{3}$$

The coefficients c_{ij} are the elements of the stiffness tensor in Voigt notation and ρ denotes the density. The dimensionless parameters ϵ and δ describe the deviation of the anisotropic traveltime isochrone from the respective isotropic traveltime isochrone, and consequently they vanish for isotropic media.

Based on the Thomsen notation (Thomsen 1986) and following Alkhalifah (1998, 2000) the phase velocity of *P*-waves for all directions in VTI media can be described by the so-called pseudo acoustic approximation

$$v_P^2(\theta) = \frac{v_{ell}^2}{2} + \sqrt{\frac{v_{ell}^4}{4} - 2(\epsilon - \delta)v_{P0}^4 \sin^2\theta \cos^2\theta}, \tag{4}$$

where v_{ell} represents the *P*-wave phase velocity in elliptical media ($\epsilon = \delta$). Due to the rotational symmetry of TI media, the phase velocity can be sufficiently described by only one (phase) angle θ. The pseudo acoustic approximation (4) is implemented by Riedel (2016) in his anisotropic eikonal solver and yields more accurate traveltimes than Thomsen's approximation for weak anisotropy, especially for stronger degrees of anisotropy.

3.5 Application of 3-D KPSDM

The traveltime calculation and the subsequent Kirchhoff pre-stack depth migration was carried out for each line separately in a 3-D volume around it. The lateral extent of the respective 3-D volume is displayed in Fig. 2 and the vertical extent of each volume was 10 km. The calculation of the traveltimes was performed within this volume on a equidistant grid with a grid spacing of 10 m. The pre-stack depth migration was carried out for the same volume but traveltimes were interpolated to a grid with 1 m grid spacing in *z*-direction (depth). We migrated from topography, that is we used the true coordinates of the receivers and sources including the significant topography. Thus, no CDP line was defined and the images in the following

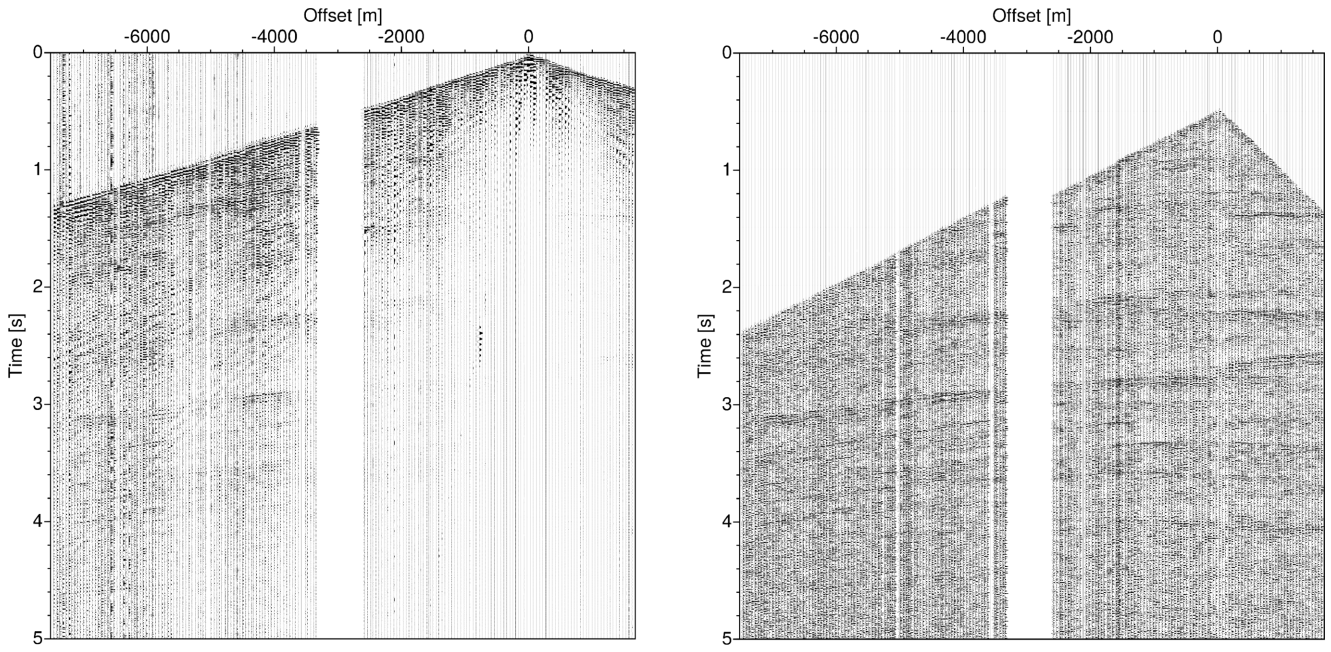

Figure 3. Left-hand panel: example of a raw shot gather from line 2. Several clear reflections are visible up to 4 s two-way traveltime. Right-hand panel: the same shot gather processed according to the parameters given in Table 2. The reflections stand out much clearer and can be traced over the entire offset range. Additionally, several previously obscured reflections are visible now.

sections represent slices through the migrated volumes. Every single pre-processed shot gather was migrated separately and afterwards the absolute migrated wavefield amplitudes were stacked to obtain the final depth migrated volume. The stacking of absolute values instead of a phase-consistent stacking method, provides a robust and adequate approach by avoiding destructive interference of the reflected signal, for example in the case of strongly heterogeneous media, which are typical for crystalline environments.

4 RESULTS

4.1 Comparison between isotropic and anisotropic depth migration

First, we present a comparison of the depth migration results using the introduced anisotropic velocity model (see Section 3.3) and a result using the corresponding isotropic velocity model, that is with the same vertical velocity function v_{P0} but with Thomsen parameters $\epsilon = \delta = 0$. Fig. 4 illustrates this comparison by showing a slice through the final migrated volume of line 3, using isotropic (left-hand panel) and anisotropic (right-hand panel) traveltimes. Both images are dominated by strong and clear reflectors, however they appear significantly more continuous and better focused in the anisotropic result. This is especially the case for the reflector at the bottom of the borehole COSC-1 at a depth of approximately 2 km. This reflector also moves downward in the anisotropic result. This is because the displayed slice through the migrated volume, due to the crooked line symmetry, does not necessarily cut through the apex of the traveltime ellipsoids that contribute to this reflection. The slice shown here is the neareast to the borehole COSC-1 and therefore not directly in the middle of the migrated volume. The positive value of δ in the anisotropic velocity model ensures that the traveltimes runs ahead the isotropic traveltimes for the near vertical directions, and therefore the mentioned reflector at approximately 2 km depth appears at a deeper position in the anisotropic migration result. Also, the horizontal reflector at a depth of 8 km is better focused in the anisotropic image and is now clearly visible as a double reflector, while in the isotropic result the reflector appears more like one blurry reflector band. Furthermore, the entire anisotropic image appears clearer and the incoherent noise is significantly reduced in comparison to the isotropic image.

To further validate the anisotropic velocity model, we calculated common image gathers (CIG), produced using the isotropic and the anisotropic velocity model for line 3 at the position of the borehole COSC-1. They are displayed in Fig. 5. In addition, we summmed over all traces of the CIGs (i.e. all offsets) and plotted this summed trace (for better visualization 5 times) next to the respective CIG. Although only limited offset ranges and only a few continuous reflectors are available, the CIGs clearly validate the anisotropic model. In the CIG for the anisotropic velocity model, the double reflector at a depth of approximately 8 km is imaged horizontally over the entire available offset range, while this reflector in the CIG for the isotropic model is only imaged for a certain offset range and is also not entirely flat. That is also the reason, why this reflector appears more blurry in the migration result (Fig. 4). In the summed trace next to the CIG, additionaly a few more reflectors are visible for the anisotropic case.

4.2 Anisotropic pre-stack depth migration results

In the following section we present the migration results for all three surface profiles. The data were pre-processed as described in Section 3.2 and we used the anisotropic 3-D Kirchhoff pre-stack depth migration approach introduced in Sections 3.4–3.5. For each profile we present the slice through the migrated volume which is nearest to the COSC-1 borehole. For the lateral extent of the migrated volumes see Fig. 2.

The final stacked migration result of the eight shots from line 1 is displayed in Fig. 6. Note that the shot positions are all located at the southwestern end of line 1. Despite the sparse and unevenly

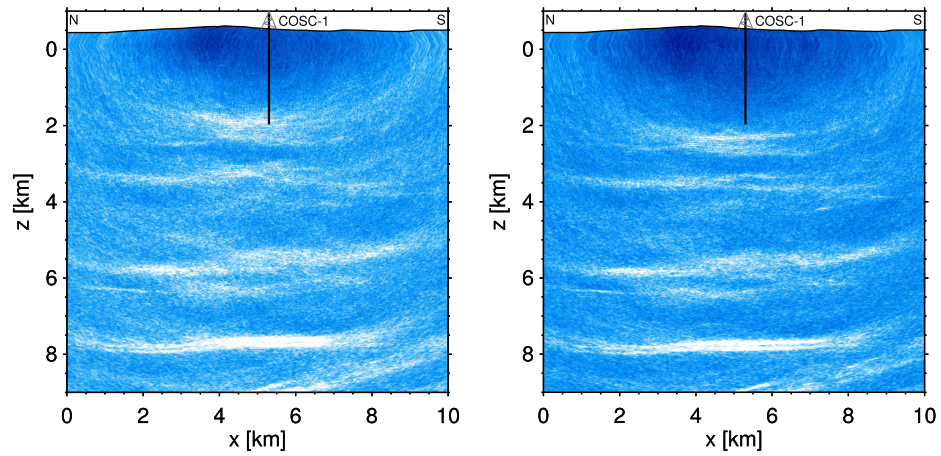

Figure 4. Kirchhoff pre-stack depth migration results for line 3, using an isotropic (left-hand panel) and anisotropic velocity model (right-hand panel) for the calculation of traveltimes. The anisotropic model is described by a 1-D vertical velocity functions v_{P0} and the Thomsen parameters $\epsilon = 0.03$ and $\delta = 0.3$ (see Section 3.3) and the corresponding isotropic model consists of the same vertical velocity function but with Thomsen parameters $\epsilon = \delta = 0$. The reflectors appear significantly more continuous and better focused in the anisotropic result.

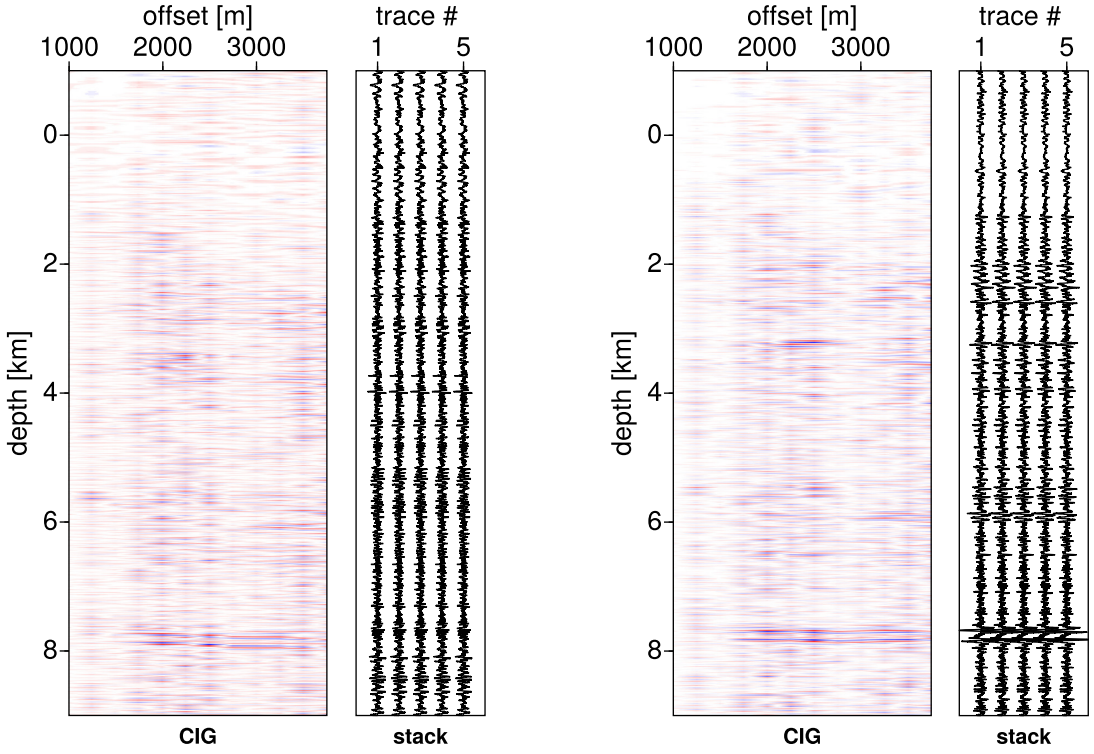

Figure 5. Common image gathers at the position of the borehole COSC-1 for line 3 for the isotropic (left-hand panel) and anisotropic velocity model (right-hand panel). In addition, a stack over all traces in the CIG is plotted next to the respective CIG (for better visualization five times next to each other.) The CIGs clearly validate the anisotropic velocity model. For the anisotropic case the reflectors appear entirely flat over the available offset range and show high amplitudes in the summed trace.

distributed shot positions, the image is dominated by clear (sub-)horizontal reflectors. Because of the limitations in the acquisition symmetry these reflectors cannot continuously be traced along the entire profile length. The uppermost reflector appears at the lower part of the borehole at 1.5 km depth. This reflector is imaged only over a small lateral extent (approximately 500 m) in the central part of the profile near the borehole. Similarly, two short reflector elements are imaged at 2.5 and 3 km depth, respectively. At about 3.5–4.0 km depth we find a slightly southwest dipping reflector, visible between $x = 1$ km and $x = 3$ km along the profile. At the southwestern end of the profile three short subhorizontal reflector elements are imaged at depths between 4.5–6.0 km. At 6.0–6.5 km depth another southwest dipping reflector is visible within a small part of the profile. The most prominent feature in this image is probably a double reflector at a depth of about 8 km, which is clearly visible along almost the entire profile length.

The migration result for line 2 is displayed in Fig. 7. On this profile, the 22 shot positions are located in the central southeastern part between approximately $x = 6.5$ km and $x = 8$ km. Due to the missing shots within the first kilometres of the profile, only the

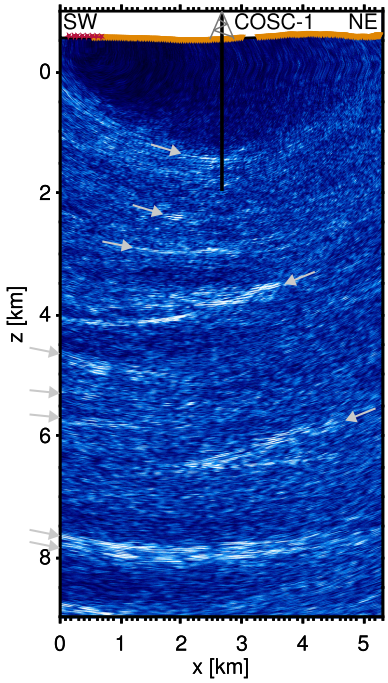

Figure 6. Anisotropic Kirchhoff pre-stack depth migration result for line 1. Shot and receiver positions are marked in red and orange, respectively. Imaged structures are indicated by arrows.

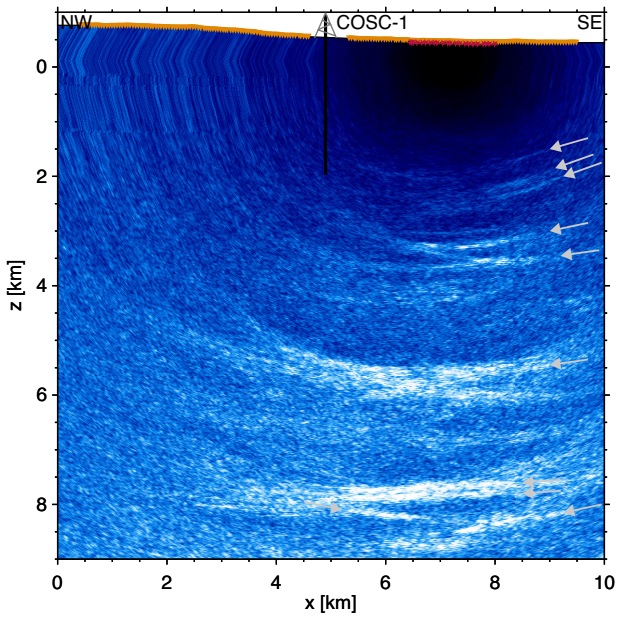

Figure 7. Anisotropic Kirchhoff pre-stack depth migration result for line 2. Shot and receiver positions are marked in red and orange, respectively. Imaged structures are indicated by arrows.

southeastern part of the profile could be imaged properly. Especially the structures in the upper approximately 4 km are visible only to a small lateral extent. The deeper structures are traceable throughout the entire profile. Nevertheless, the reflectors stand out very clearly. The uppermost reflectors are three short, rather weak, northwest dipping elements between 1.5 and 2.5 km depth. At a depth of 3.0 and 3.5 km two more reflector elements appear. Between 5 and 6 km depth a more blurry reflector is imaged between $x = 4.0$ km and $x = 9.0$ km along the profile. At about 8 km depth a double reflector similar to line 1 is imaged. Below this double reflector some shorter slightly southeast and northwest dipping elements are visible.

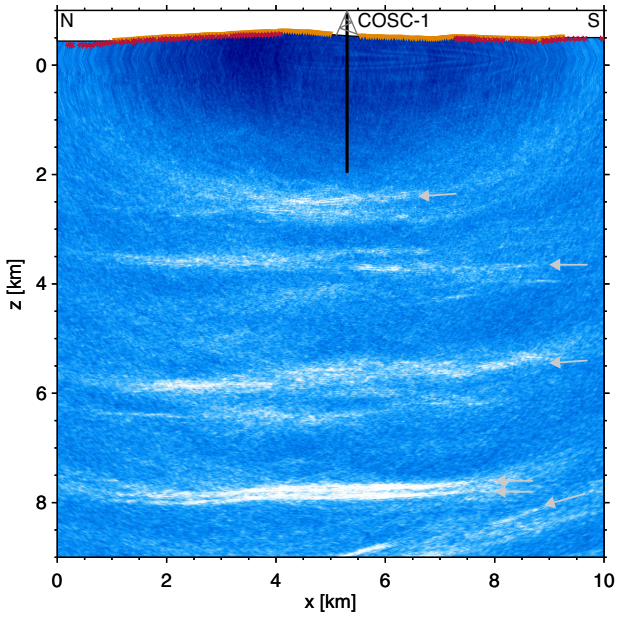

Figure 8. Anisotropic Kirchhoff pre-stack depth migration result for line 3. Shot and receiver positions are marked in red and orange, respectively. Imaged structures are indicated by arrows.

Fig. 8 shows the migration result along line 3. Along this profile the shot positions are more evenly distributed, only in the central southern part a bigger gap exisists. Therefore, also the imaged structures are more continuous along the entire profile. Overall, four main structures are imaged along line 3. All of them are horizontal to subhorizontally dipping to the north. The uppermost reflection is located directly below the borehole COSC-1 at a depth of approximately 2.5 km. Directly below a double reflector can be observed at a depth of approximately 3.5 km. Between 5.5 and 6.0 km depth a slightly north dipping reflector is visible. The most prominent feature is again the bright and continuous double reflector at a depth of 8 km. Below, some north dipping reflector elements can be found between $x = 5$ km and $x = 10$ km along the profile.

A 3-D view of the final anisotropic imaging results for all three lines is displayed in Fig. 9. The three profiles were centred around the COSC-1 borehole and they show a good agreement in the position of the imaged structures where they intersect each other, although they were acquired and processed independently from each other.

5 INTERPRETATION AND COMPLEMENTARY RESULTS

As already described in Section 2.2, the area of the central Scandinavian Caledonides around the COSC-1 borehole is well examined through various seismic studies performed during the last decades. These investigations range from the crustal scale Central Caledonian Transect (CCT) profile over the more regional COSC Seismic Profile (CSP), a high-resolution 3-D and VSP surveys to small scale borehole logs and drill core measurements of seismic properties. The depth imaging of the three long offset surface profiles centred on the COSC-1 borehole in this study, provides a link regarding survey geometry and resolution between the regional 2-D COSC

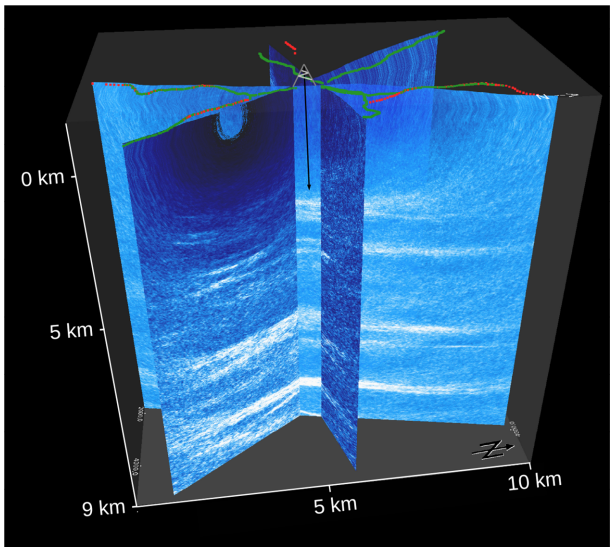

Figure 9. 3-D view of anisotropic pre-stack depth migration results of the three independently processed surface profiles. The shot and receiver positions are marked in red and green, respectively.

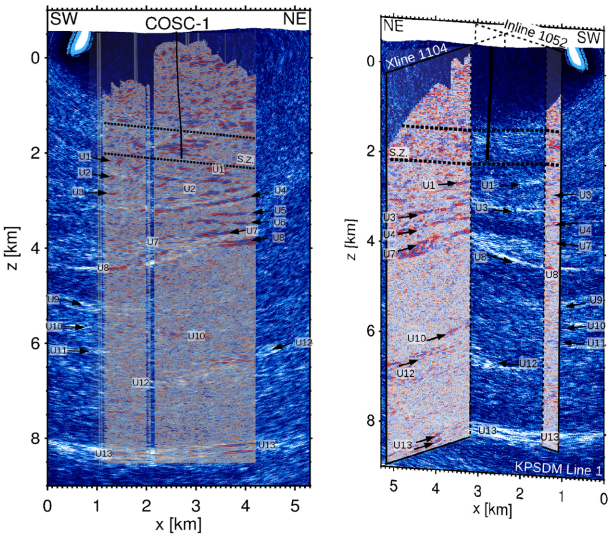

Figure 10. Comparison between anisotropic KPSDM of line 1 and 3-D data processed by Hedin *et al.* (2016) and depth converted by Krauß (2018). Left-hand panel: Line 1 overlayed by the corresponding slice through the 3-D volume. No-fold parts of the 3-D volume are made transparent and opacity is lowered. Right-hand panel: 3-D view from west–northwest, showing line 1 in comparison to inline 1052 and crossline 1104 of the 3-D volume. A major shear zone (S.Z.) is indicated at the lower part of the borehole COSC-1 and below many clear reflector elements (U1-U13) can be traced throughout line 1 and the 3-D volume.

Seismic Profile and the high-resolution 3-D survey in the direct vicinity around the COSC-1 borehole. In the following the results of our Kirchhoff pre-stack depth migration are therefore discussed and interpreted in comparison to the CSP (Juhlin *et al.* 2016) and the 3-D data (Hedin *et al.* 2016) in order to further support the geological interpretation of the area.

Due to different (although similar) velocity models used for depth conversion or depth migration and different processing steps, the three data sets used for the comparison are not exactly comparable, especially regarding the depth of the structures. The time to depth conversion of the post stack time migrated CSP was carried out with a smoothed velocity function based on the velocity analysis of the data set (Juhlin *et al.* 2016). For the 3-D data a 1-D velocity function was used for depth conversion, which was based on averaged velocities from zero-offset VSP and extended below the borehole COSC-1 with an assumed constant gradient up to 6100 m s^{-1} at 9000 m depth (Hedin *et al.* 2016). Krauß (2018) introduced a slightly different depth conversion for the uppermost 2.5 km of the 3-D data. The latter is more similar to the velocity function used in our anisotropic velocity model and we therefore used this depth converted 3-D data set for the comparison.

At first, we compare our migration result for line 1 with the corresponding slice through the 3-D volume as well as a representative inline (Inline 1052) and crossline (Xline 1104) of the latter from different view points (Fig. 10). Furthermore, we compiled a 3-D view of line 1, line 2, inline 1052 through the 3-D data and the northwestern part of the CSP (Fig. 11), and a comparison of line 3 with the corresponding slice through the 3-D volume and the CSP viewed from northeast (Fig. 12). The numbering of the imaged structures below the SNC by U1–U8 within Figs 10-12 is in accordance to Hedin *et al.* (2016). Here we extended this numbering for the deeper structures up to U14.

The uppermost approximately 2.5 km, interpreted as the Seve Nappe Complex (Hedin *et al.* 2012, 2016; Juhlin *et al.* 2016) appear as a highly reflective unit with very patchy internal structures in the CSP. The 3-D data revealed a complicated 3-D structure with low lateral continuation of the reflectors that are dipping in different directions. In the eastern part the boundary of the SNC could be clearly defined as a gently west-dipping reflector, but the boundary below the central part remains diffuse. In our pre-stack depth migration results the SNC appears seismically transparent. This can be explained by the limitations in the acquisition geometry, a significantly smaller number of sources and receivers as well as a larger shot and receiver spacing. It might also be due to our processing of the data, which focused on deeper structures. Therefore, the results by Hedin *et al.* (2016) focusing on the shallower parts provide a good image and interpretation of the SNC and the directly underlying units, while we complement this by concentrating also on deeper structures below the SNC.

Below 1710 m depth mylonite bands occur in the COSC-1 drill core with increasing frequency (Lorenz *et al.* 2015), which is an indication for increasing strain in this part of the SNC. Therefore, the thick and well defined reflectivity band that is visible in the 3-D data and to a smaller extent in the depth migration result of line 1 (Fig. 10) at the base of the borehole COSC-1 at a depth of around 1.5 km is interpreted by Hedin *et al.* (2016) as a basal shear zone (S.Z. in Fig. 10) of the SNC. Within this zone a borehole intersecting reflector is imaged in the depth migration result for line 1. It is hard to judge which observation from the core exactly causes this reflector due to strong interlayering of different lithologies with often only few metres of thickness, which is not observable with the measured seismic frequencies. Probably one or a superposition of several mylonites causes this reflector. The shear zone has a thickness of approximately 1 km and is underlain by the reflector U1 that could be imaged only to a very small extent in our results of line 1 due to the already mentioned limitations in recording geometry. This reflector appears to dip eastward in the 3-D volume. U1, together with the parallel eastwards dipping reflector U2, are interpreted as the boundaries of the Särv/Offerdal Nappes, which outcrop on the surface at the western margin of the SNC (see Fig. 1) but which are hardly traceable at the eastern side of the SNC. This suggests, that the Särv/Offerdal Nappes are very thin, probably not

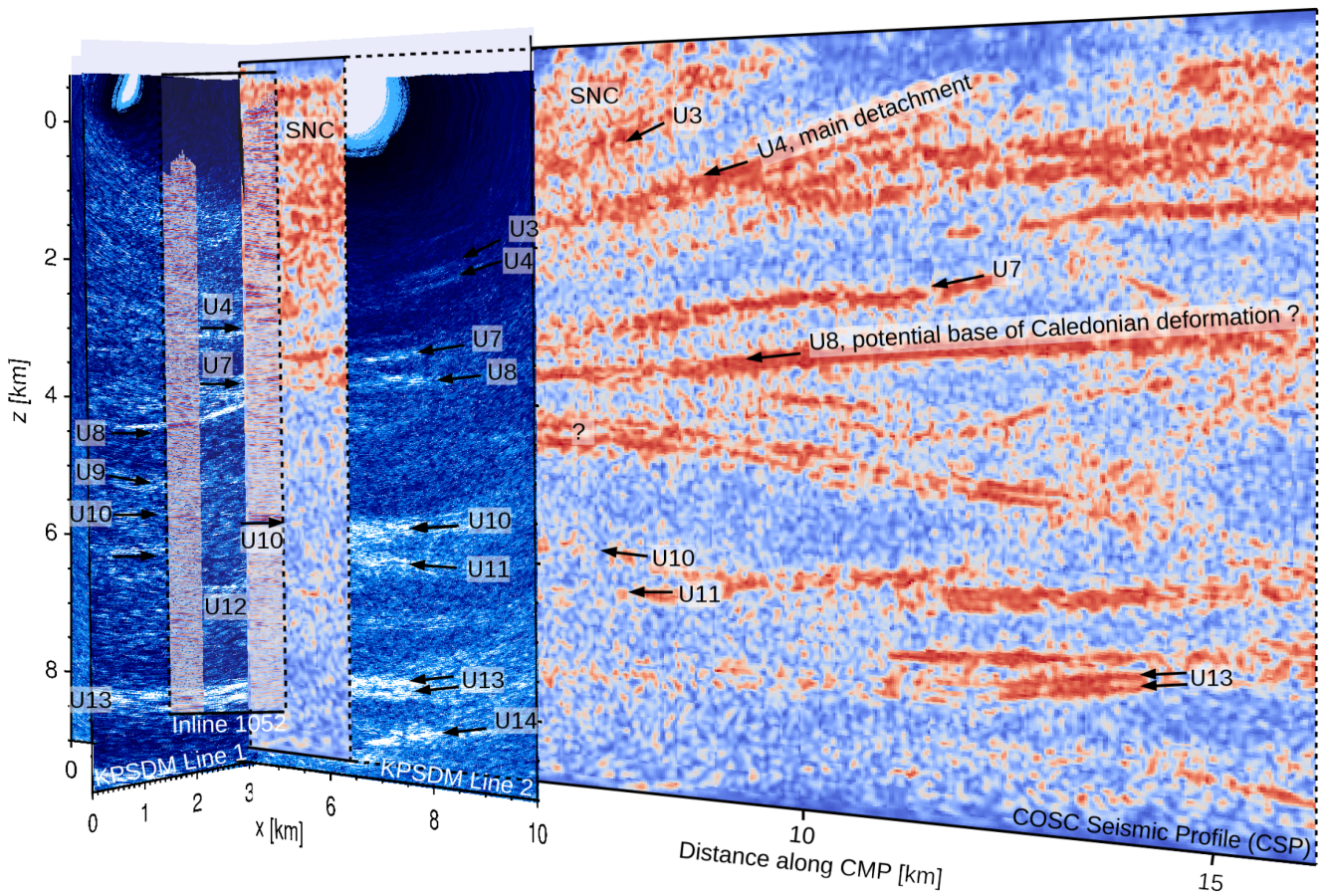

Figure 11. 3-D view of line 1, line 2, inline 1052 through the 3-D volume (processed by Hedin *et al.* (2016) and depth converted by Krauß (2018)) and the north-eastern part of the CSP (Juhlin *et al.* 2016) viewed from south. No-fold areas of the 3-D volume are made transparent. Many clear reflectors can be traced (more or less continuous) throughout all three data sets. But also some differences are found regarding the deeper structures (U9–U14) that are less visible in the CSP and the 3-D data, especially below the Seve Nappe Complex (SNC).

continuous and pinch out underneath the SNC somewhere in the Åre Synform.

Both reflectors U1 and U2 are terminated by U3, a subhorizontal strong reflector at a depth of 3 km, especially visible in the migration result of line 1 and crossline 1104 in Fig. 10 but also weakly at the south-eastern end of line 2 (Fig. 11) where it becomes slightly north-dipping. U3 defines, together with U1 in the west, the base of the Seve Nappes. In the 3-D data this reflector appears at the top of a several hundred metres thick reflective zone and is interpreted as the top of the Lower Allochthons (ordovician turbidites, limestones and alum shales), that are bounded at their base by the reflector U4. The latter was interpreted by Hedin *et al.* (2016) as the main décollement, that separates the long-transported Jämtlandian allochthons from the underlying less deformed Precambrian crystalline basement. Reflector U4 is not or only weakly imaged (for example in line 2, Fig. 11) in the pre-stack depth migration results of the three lines. Alternatively, the supposed reflector indicated as U3 in the line 1 result actually is U4. This is not completely clear and hard to interpret due to the different velocity models and the consequently slightly different depths of the reflectors. However, this reflector can be traced clearly in the CSP (see Figs 11 and 12) at a depth of around 3 km below the SNC and then rising towards shallower depths of about 0.5 km in the east.

U5 and U6 are only visible within small parts of the 3-D volume (e.g. the slice through the 3-D volume which is parallel to line 1, Fig. 10), but not in the pre-stack depth migration results of the three surface profiles. They are probably related to allochthonous basement derived units, which is also supported by geological mapping along the major antiforms west and east the Åre Synform (Hedin *et al.* 2016).

The deeper prominent reflections U7 and U8 are interpreted by Hedin *et al.* (2016) as subparallel and horizontal. It appears on line 1 that U8 is dipping with approximately 15° to southwest and ramps up into U7 (see Figs 10 and 11). Both, U7 and U8 can clearly be traced throughout all three profiles and can be followed also far into the southeastern extension of line 2, the CSP (see Fig. 12). According to Hedin *et al.* (2016) and Juhlin *et al.* (2016) the very prominent U8 reflector may represent the base of Caledonian deformation or sole thrust. This thrust zone defines the lower limit of Caledonian deformation, including allochthons and basement. Nevertheless, also deeper Caledonian deformation cannot be excluded. Further east, near the thrust front, the potential sole thrust ramps up into the main décollement, denoted here as U4 (Juhlin *et al.* 2016). To the west, the sole thrust continues gently dipping until the Swedish-Norwegian border, where it reaches a depth of approximately 7 km (Hurich *et al.* 1989).

The subhorizontal elements U9–U12 are visible with various extent throughout the different data sets. U9 can be found only at the southwestern end of line 1, as a short slightly northeast dipping element, but it is not visible in any of the other data sets. U10

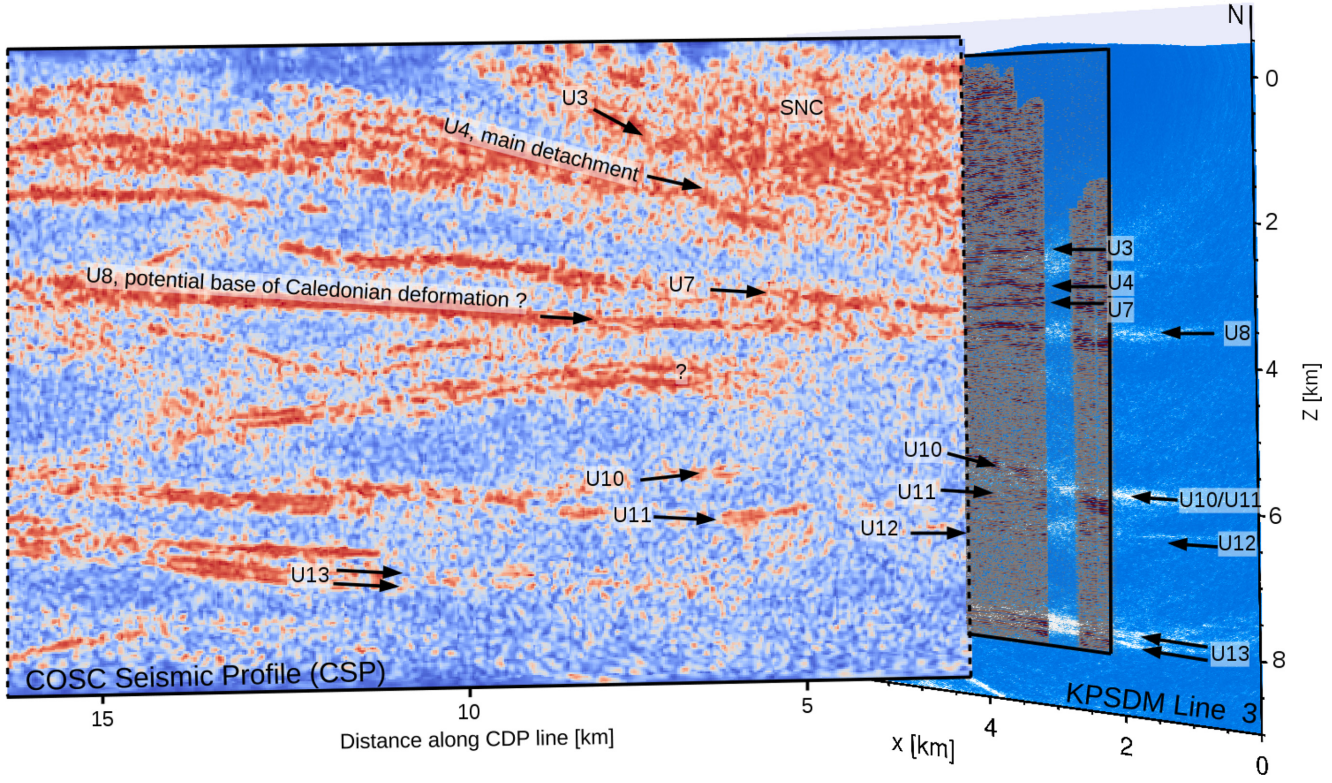

Figure 12. 3-D view of line 3, the corresponding slice through the 3-D volume (processed by Hedin *et al.* (2016) and depth converted by Krauß 2018) and the northeastern part of the CSP (Juhlin *et al.* 2016) viewed from east–northeast. No-fold areas of the 3-D volume are made transparent. Many clear reflectors can be traced (more or less continuous) throughout all three data sets. But also some differences are found regarding the deeper structures (U9–U14) that are less visible in the CSP and the 3-D data, especially below the Seve Nappe Complex (SNC).

appears subhorizontal to slightly dipping towards northeast in line 1 and the corresponding slice through the 3-D volume (Fig. 10) as well as in crossline 1104 and line 2 and line 3 (Figs 11 and 12). Beginning from line 2 it can be followed almost continuously into the CSP, where it has a slightly southeast dipping component (Fig 11) and merges with reflector U11. The latter can be traced back via line 2 and line 1 (Fig. 11) where it seems that U10 and U11 again merge right below the borehole COSC-1. U12 is found in line 1 and crossline 1104 (Fig. 10) as well as in line 3 (Fig. 12) as a southwest dipping strong reflector, but no corresponding reflector is visible in the CSP.

The most prominent deep structure is a strong and continuous horizontal double reflector (U13) at about 8.0–8.5 km depth, which is clearly visible in the depth migration results of the three surface lines, but less continuous and weaker in the 3-D volume. Further southeast in the CSP a similar double reflector can be found at the same depth, which is interpreted as the continuation of this prominent feature.

In line 2 an additional shorter northwest dipping element below the double reflector is imaged (Fig. 11), but no corresponding similar element can be found in any of the other data sets.

Since no information below the borehole is available that can provide clues on the structures, the observed strong reflections from within the Precambrian basement (everything below U4) remain enigmatic. Different scenarios have been discussed, about what could cause this strong reflectivity from within the basement (e.g. Palm *et al.* 1991; Juhojuntti *et al.* 2001). One reason could be the intrusion of mafic dykes into the dominantly granitic basement. In the Siljan Ring, about 100 km southeast, dolerite sills are drilled, which produce a similar seismic response (Juhlin 1990). Also surface outcrops of 0.95 and 1.25 Ga dolerite dykes are found south and east of the Caledonian thrust front. Another explanation are deformation zones, developed during the Caledonian or the (Precambrian) Sveconorwegian orogeny. During the Caledonian orogeny, the Baltica basement probably experienced an eastward progressing deformation during the nappe emplacement towards the foreland. Therefore, it is likely, that at least some of the deep reflections represent deformation zones.

6 CONCLUSIONS

The anisotropic Kirchhoff pre-stack depth migration approach provides images with clear and dominant reflections down to a depth of 9 km. Despite the irregular and partly sparse acquisition geometry, especially regarding the distribution of the source points, the imaged structures are mostly well defined. The use of anisotropic Green's functions for the depth migration that are calculated from a VTI velocity model, significantly improved the quality of the imaged reflectors. They appear better focused and more continuous in comparison to depth migration images using the corresponding isotropic traveltimes. This suggests that anisotropy, when it is present and well defined, should be considered also for seismic imaging in crystalline environments. Here, the anisotropic velocity model was constructed by the combined analysis of surface and borehole data and laboratory measurements on core samples (Simon *et al.* 2017).

The analysis of the three seismic profiles that are centred on the COSC-1 borehole fills a gap between the high-resolution 3-D data in

the direct vicinity of the borehole and the more regional scale COSC Seismic Profile (CSP) that was used to define the drill locations. Many of the reflectors can be traced throughout all three lines and additionally linked to previously known structures in the 3-D data set (Hedin *et al.* 2016) and the CSP (Juhlin *et al.* 2016). Therefore, this analysis basically supports the interpretation made from the 3-D data and the CSP. The uppermost 2 km appear seismically transparent, which is in clear constrast to the 3-D data and the CSP where a highly reflective unit with complicated internal structure was interpreted as the Seve Nappe Complex (SNC). The difference is probably due to the limitations in the acquisition geometry (e.g. receiver spacing of 50 m, irregular and partly sparse distribution of source points) but might also be due to the processing. Nevertheless, the shear zone in the lower part of the SNC could be imaged as well as the reflectors at the base of the SNC, probably defining different units in the Middle and Lower Allochthons. The main décollement that separates the (Jämtlandian) allochthons from the underlying basement at about 3 km depth is more difficult to detect in our migration results than in the 3-D data. Due to different velocity models used for depth conversion and migration it is not exactly clear in this part of the images which reflector can be linked to the structures in the 3-D data. In the deeper parts it is more obvious and the dominant reflectors can clearly be linked and followed for large distances in the CSP, like the U8 reflector which may indicate the base of the potential Caledonian deformation. The most prominent feature in all three profiles is a double reflector at a depth of about 8 km, which has its equivalent further to the southeast in the CSP at a similar depth. The deeper reflections appear more dominant than in the 3-D data and the CSP. In the latter they are mostly not even visible below the SNC. Nevertheless, the origin of the reflectivity from within the basement remains enigmatic and might be clarified through the drilling of COSC-2, which is supposed to penetrate at least one of the basement reflectors. The presently discussed scenarios are deformation zones of Caledonian or pre-Caledonian age or deformed mafic (dolerite) intrusions into the dominantly granitic basement.

ACKNOWLEDGEMENTS

We thank the German Research Foundation (DFG, grants BU1364/10-1 and GI982/2-1) for funding this project within the Priority Program ICDP (SPP 1006). The Geophysical Instruments Pool Potsdam (GIPP) provided the surface geophones and wireless recorders for the three surface profiles. The pre-processing of the data was mainly carried out using the Software SeisSpace/ProMAX, for which we gratefully acknowledge the support by the Halliburton-Landmark Software Grant. We particularly thank all members of the field crew for their excellent work during the survey. We are particularly grateful to the reviewers and editor for their valuable and constructive comments, which significantly improved the paper.

REFERENCES

Alkhalifah, T., 1998. Acoustic approximations for processing in transversely isotropic media, *Geophysics,* **63**(2), 623–631.

Alkhalifah, T., 2000. An acoustic wave equation for anisotropic media, *Geophysics,* **65**(4), 1239–1250.

Andersen, T., 1998. Extensional tectonics in the Caledonides of southern Norway, an overview, *Tectonophysics,* **285,** 333–351.

eds Corfu, F., Gasser, D. & Chew, D.M., 2014. *New Perspectives on the Caledonides of Scandinavia and Related Areas,* Geological Society, London, Special Publications 390.

Cosma, C. & Enescu, N., 2001. Characterization of fractured rock in the vicinity of tunnels by the swept impact seismic technique, *Int. J. Rock Mech. Mining Sci.,* **38**(6), 815–821.

Dyrelius, D., Gee, D., Gorbatschev, R., Ramberg, H. & Zachrisson, E., 1980. A profile through the central scandinavian caledonides, *Tectonophysics,* **69**(3-4), 247–284.

Gee, D., 1975. A tectonic model for central part of Scandinavian Caledonides, *Am. J. Sci.,* **275-A,** 468–515.

Gee, D., 1978. Nappe displacement in Scandinavian Caledonides, *Tectonophysics,* **47**(3-4), 393–419.

eds Gee, D. & Sturt, B., 1985. *The Caledonide Orogen - Scandinavia and Related Areas,* John Wiley & Sons Ltd.

Gee, D., Fossen, H., Henriksen, N. & Higgins, A., 2008. From the early Paleozoic platforms of Baltica and Laurentia to the Caledonide orogen of Scandinavia and Greenland, *Episodes,* **31**(1), 44–51.

Gee, D., Juhlin, C., Pascal, C. & Robinson, P., 2010. Collisional Orogeny in the Scandinavian Caledonides (COSC), *GFF,* **132**(1), 29–44.

Hedin, P., 2015. Geophysical studies of the upper crust of the central Swedish Caledonides in relation to the COSC scientific drilling project, *PhD thesis*, Uppsala University.

Hedin, P., Juhlin, C. & Gee, D., 2012. Seismic imaging of the Scandinavian Caledonides to define ICDP drilling sites, *Tectonophysics,* **554-557,** 30–41.

Hedin, P. *et al.*, 2016. 3D reflection seismic imaging at the 2.5 km deep COSC-1 scientific borehole, central Scandinavian Caledonides, *Tectonophysics,* **689,** 40–55.

Hurich, C., Palm, H., Dyrelius, D. & Kristoffersen, Y., 1989. Deformation of the Baltic continental crust during Caledonide intracontinental subduction: views from seismic reflection data, *Geology,* **17**(5), 423.

Juhlin, C., 1990. Interpretation of the reflections in the Siljan Ring area based on results from the Gravberg-1 borehole, *Tectonophysics,* **173**(1-4), 345–360.

Juhlin, C., Dehghannejad, M., Lund, B., Malehmir, A. & Pratt, G., 2010. Reflection seismic imaging of the end-glacial Pärvie Fault system, northern Sweden, *J. appl. Geophys.,* **70**(4), 307–316.

Juhlin, C., Hedin, P., Gee, D., Lorenz, H., Kalscheuer, T. & Yan, P., 2016. Seismic imaging in the eastern Scandinavian Caledonides: siting the 2.5 km deep COSC-2 borehole, central Sweden, *Solid Earth,* **7,** 769–787.

Juhojuntti, N., Juhlin, C. & Dyrelius, D., 2001. Crustal reflectivity underneath the Central Scandinavian Caledonides, *Tectonophysics,* **334**(3-4), 191–210.

Korja, T., Smirnov, M., Pedersen, L.B. & Gharibi, M., 2008. Structure of the Central Scandinavian Caledonides and the underlying Precambrian basement, new constraints from magnetotellurics, *Geophys. J. Int.,* **175**(1), 55–69.

Krauß, F., 2018. Combination of Borehole Seismic and Downhole Logging to Investigate the Vicinity of the COSC-1 Borehole in Western Scandinavia, *PhD thesis,* TU Bergakademie Freiberg.

Lorenz, H. *et al.*, 2015. COSC-1 - drilling of a subduction-related allochthon in the Palaeozoic Caledonide orogen of Scandinavia, *Scient. Drilling,* **19,** 1–11.

Palm, H., Gee, D., Dyrelius, D. & Björklund, L., 1991. A Reflection seismic image of Caledonian structure in central Sweden, *Sveriges Geologiska Undersökning,* **75**(75), 1–36.

Park, C., Miller, R., Steeples, D. & Black, R., 1996. Swept impact seismic technique (SIST), *Geophysics,* **61**(6), 1789–1803.

Podvin, P. & Lecomte, I., 1991. Finite-difference computation of traveltimes in very contrasted velocity models—a massively parallel approach and its related tools, *Geophys. J. Int.,* **105**(1), 271–284.

Riedel, M., 2016. Efficient computation of seismic traveltimes in anisotropic media and the application in pre-stack depth migration, *PhD thesis,* TU Bergakademie Freiberg.

Sethian, J., 2001. Evolution, implementation, and application of level set and fast marching methods for advancing fronts, *J. Comput. Phys.,* **169**(2), 503–555.

Sethian, J. & Popovici, A., 1999. 3-D traveltime computation using the fast marching method, *Geophysics,* **64**(2), 516–523.

Simon, H., Buske, S., Krauß, F., Giese, R., Hedin, P. & Juhlin, C., 2017. The derivation of an anisotropic velocity model from a combined surface and borehole seismic survey in crystalline environment at the COSC-1 borehole, central Sweden, *Geophys. J. Int.,* **210**(3), 1332–1346.

Streule, M., Strachan, R., Searle, M. & Law, R., 2010. Comparing Tibet-Himalayan and Caledonian crustal architecture, evolution and mountain building processes, in *Continental Tectonics and Mountain Building - The Legacy of Peach and Horne,* pp. 207–232, eds Law, R.D., Butler, R.W.H., Holdsworth, R.E., Krabbendam, M. & Starchan, R.A., Geological Society, London, Special Publications 335.

Strömberg, A., Karis, L., Zachrisson, E., Sjöstrand, T., Skoglund, R., Lundegårdh, P. & Gorbatschev, R., 1984. Berggrundskarta över Jämtlands län utom förutvarande Fjällsjö kommun, scale 1:200 000, *Sveriges Geologiska Undersökning,* **Ca 53,** Uppsala, Sweden.

Thomsen, L., 1986. Weak elastic anisotropy, *Geophysics,* **51**(10), 1954–1966.

Wenning, Q., Almqvist, B., Hedin, P. & Zappone, A., 2016. Seismic anisotropy in mid to lower orogenic crust: Insights from laboratory measurements of Vp and Vs in drill core from central Scandinavian Caledonides, *Tectonophysics,* **692,** 14–28.

Yan, P., Garcia Juanatey, M.d.L.A., Kalscheuer, T., Juhlin, C., Hedin, P., Savvaidis, A. & Lorenz, H., 2017a. A magnetotelluric investigation of the Scandinavian Caledonides in western Jämtland, central Sweden, using the COSC-1 borehole log as a priori information, *Geophys. J. Int.,* **208,** 1465–1489.

Yan, P., Kalscheuer, T., Hedin, P. & Garcia Juanatey, M.A., 2017b. Two-dimensional magnetotelluric inversion using reflection seismic data as constraints and application in the COSC project, *Geophys. Res. Lett.,* **44**(8), 3554–3563.